Morphology of Polyvinylidene Fluoride and Its Blend in Thermally Induced Phase Separation Process

Xianfeng Li, Xiaolong Lu

Key Laboratory of Hollow Fiber Membrane Materials and Membrane Process of Ministry of Education, Tianjin Polytechnic University, Tianjin 300160, China

Received 31 August 2005; accepted 13 October 2005
DOI 10.1002/app.23489
Published online in Wiley InterScience (www.interscience.wiley.com).

ABSTRACT: Polyvinylidene fluoride (PVDF) and its blend films were prepared by melt-blending the binary mixture of PVDF/dibutyl phthalate (DBP) and the ternary mixture of PVDF/$CaCO_3$/DBP in combination of TIPS. Their morphologies were characterized by scanning electron microscope depended on preparation condition, such as the diluent and $CaCO_3$ weight fraction, and the cooling rate, and the crystallization information was also investigated by DSC. The results showed that $CaCO_3$ influenced the morphology of PVDF in the TIPS process regardless of the cooling conditions, and the formation of the spherulitic morphology can be disturbed by $CaCO_3$ at the quenching condition. The effect of $CaCO_3$ weight fraction on the tensile strength of PVDF was measured, which indicated $CaCO_3$ had a negative effect on PVDF tensile strength. © 2006 Wiley Periodicals, Inc. J Appl Polym Sci 101: 2944–2952, 2006

Key words: polyvinylidene fluoride; morphology; thermally induced phase separation; blend

INTRODUCTION

The membrane industry is interested in PVDF polymer due to its resistant to high temperature, γ-radiation, abrasion, demanding chemical environments, including acids, alkaline, strong oxidants, and halogens.[1] In fact, PVDF membrane has been extensively investigated using the traditional membrane-formation methods, such as diffusion-induced phase separation (DIPS).[1–3]

Thermally induced phase separation (TIPS) has also proven to be a valuable method for making commercial membranes and it has been studied extensively.[4–10] The porous membranes can be readily prepared in the various forms of sheets,[5] hollow fibers,[6] and tubulars[10] by TIPS process. Membrane materials focused on polypropylene (PP),[4] polyethylene (PE),[6] polystyrene (PS),[7] cellulose acetate (CA),[8] and poly(ethylene-*co*-vinyl alcohol) (EVAL).[9] The use of TIPS for the formation of PVDF porous membrane is relatively poor; some works were done by Lloyd,[11] and their study showed that PVDF/DBP solution exhibited solid/liquid phase separation, which resulted in a fuzzy sphere structure. This is an unfavorable structure for a separation membrane. Recently, some patents about PVDF membrane reported the advantages of preparing membrane from PVDF, organic liquid, and inorganic powder.[12–14]

In addition, it should also be noted that, in the process of membrane preparation by DIPS, a unique polymer/inorganic particle membrane material can be developed to enhance the properties of membranes by the addition of an inorganic particle to a polymer.[15–18]

The aim of this study is to obtain a membrane morphology database under different preparing conditions, including the introduction of $CaCO_3$ particle, to investigate the effect of the composition of the initial casting solution and the cooling conditions on the morphology of PVDF and its blend, and to provide the fundamental knowledge necessary to prepare PVDF porous membranes by TIPS in combination with blend inorganic particle.

EXPERIMENTAL

Materials

Polyvinylidene fluoride (PVDF, solef1010, melting point 177 °C) was supplied by Solvay (France); dibutyl phthalate (DBP, density 1.043 g/cm^3; boiling point 340°C) and $CaCO_3$ (average particle size <2 μm) are of industrial grade and used without further purification.

*Correspondence to:*X. Li (xianfengli@eyou.com).
Contract grant sponsor: National 973 Program; contract grant number: 2003CB615700.
Contract grant sponsor: Science Council of Tian Jin; contract grant number: 05YFJMJC04500.
Contract grant sponsor: Educational Council of Tian Jin; contract grant number: 20041402.

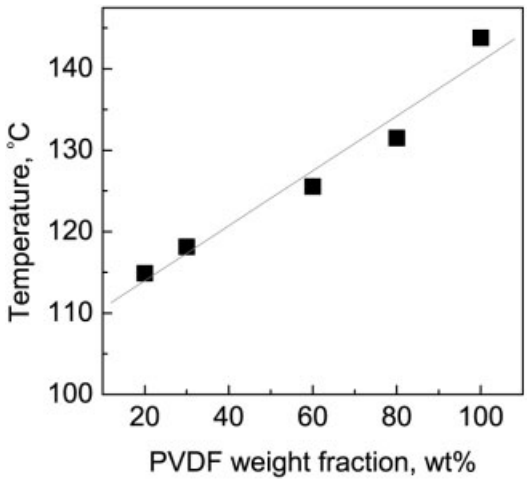

Figure 1 Crystallization temperature–concentration of PVDF.

Preparation of blend samples

PVDF/DBP binary system (I)

Blend system was weighed into a test tube with a total sample weight of 10 g, melted at 220°C, formed homogeneous solution, quenched to solidify the sample, and the formed sample materials were used for DSC test and for preparing sample membranes. The sample membranes were prepared as follows: the sample materials were sliced into small pieces, placed between two microscope glass slips, heated, formed 0.4–0.6 mm thickness films. They were solidified by two cooling rate: spontaneously cooling in the oven (cooling rate about 0.8°C/min) and (2) quenching in the 25°C water bath. The detail processes refer to the literature.[11]

PVDF/DBP/$CaCO_3$ ternary system (II)

Premixed ternary systems were further melt kneaded for 6–8 min at 220°C by torque rheometer (XSS-30, Shang Hai, China), which was used as the sample materials for preparing blend sample films by two ways: (1) preparation conditions were the same as the aforementioned binary sample film with the two cooling rate; (2) the blend sample materials were put into a mold, hot-pressed into membrane, cooled, and solidified and used for SEM and tensile strength measurement. The thickness of films is about 1 mm.

Tensile break strength measurements

The dog-bone tensile pieces (thickness 1 mm, width 6.5 mm) were prepared from blend sample II. The tests were done at room temperature using a WDW-100B tensile test machine (Changchun, China), and the ten-

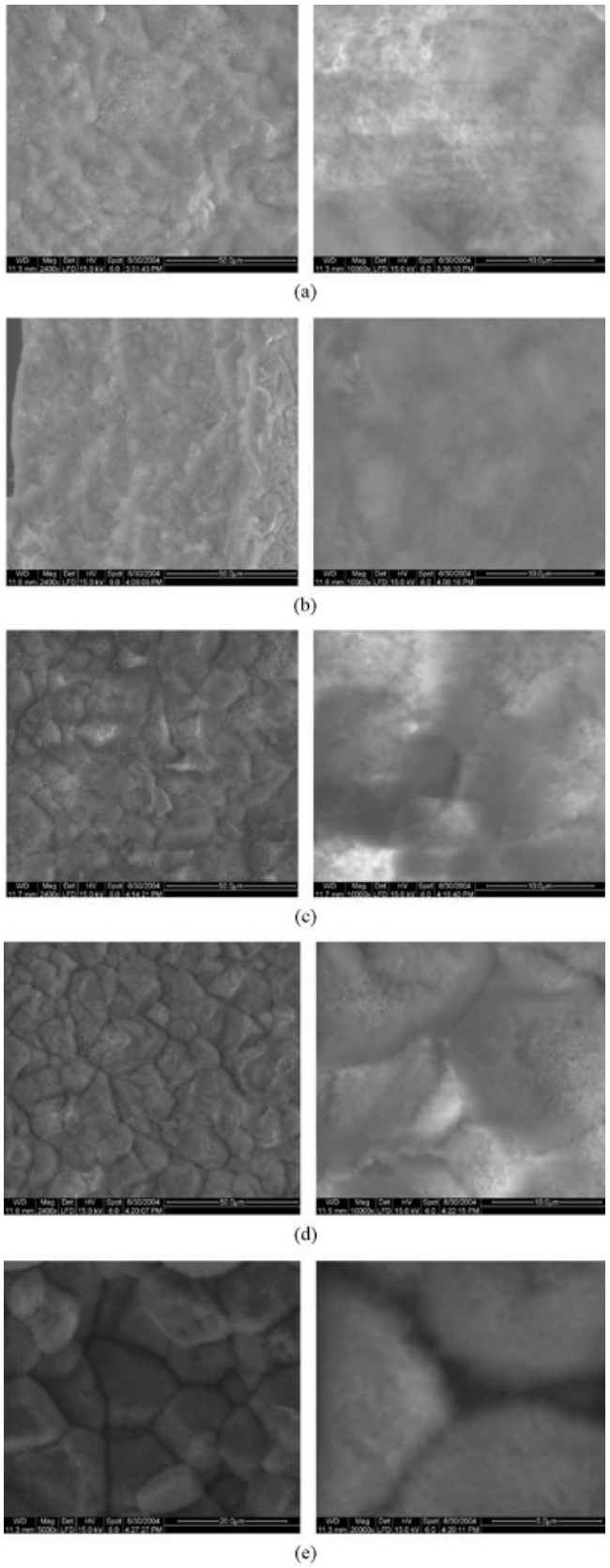

Figure 2 Effect of DBP content on the morphology of PVDF membranes, quenching at 25°C water bath (PVDF%: (a) 20%, (b) 30%, (c) 40%, (d) 50%, (e) 60%).

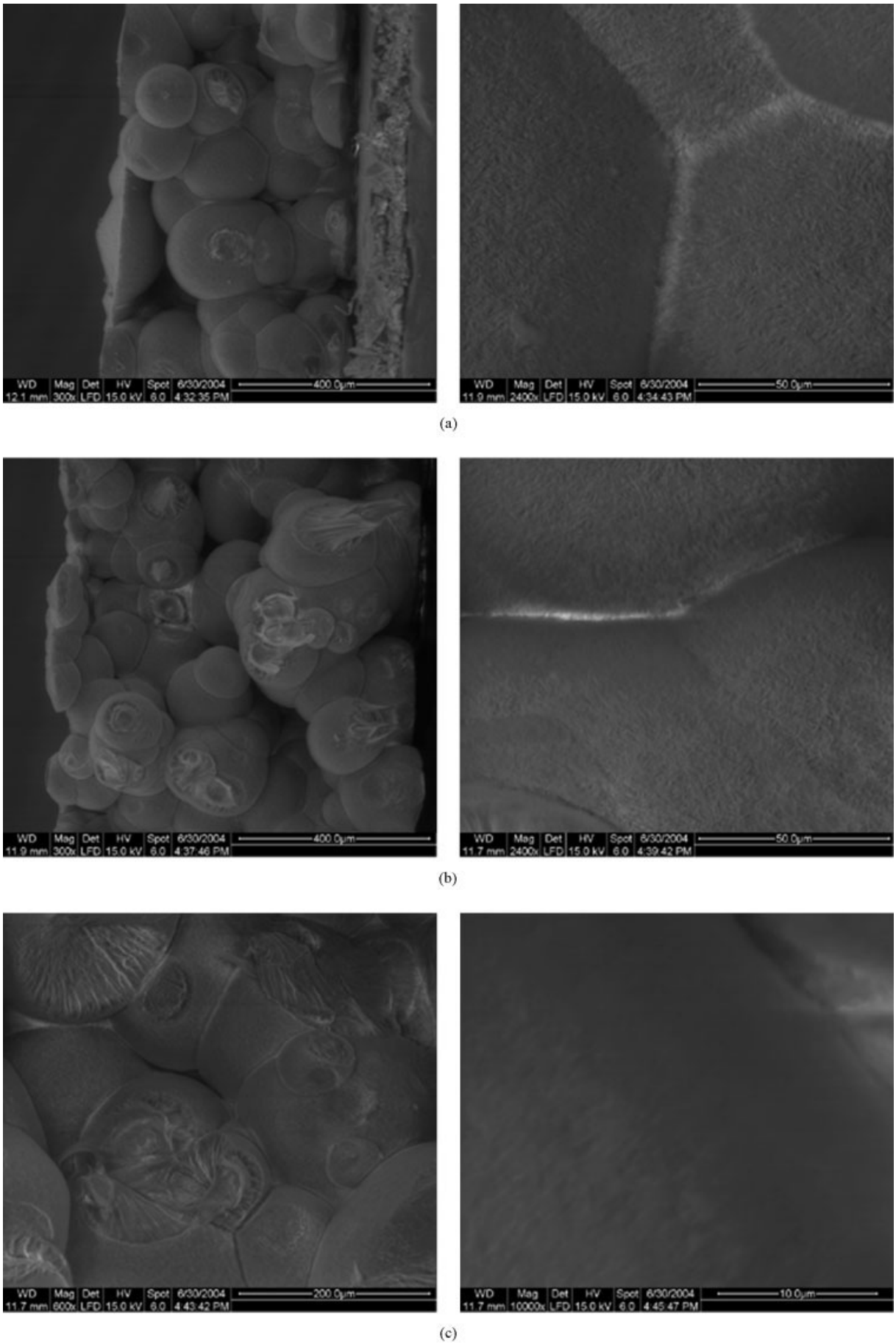

Figure 3 Morphology of PVDF membranes at about 0.8°C/min cooling rate (PVDF%: (a) 40%, (b) 50%, (c) 60%).

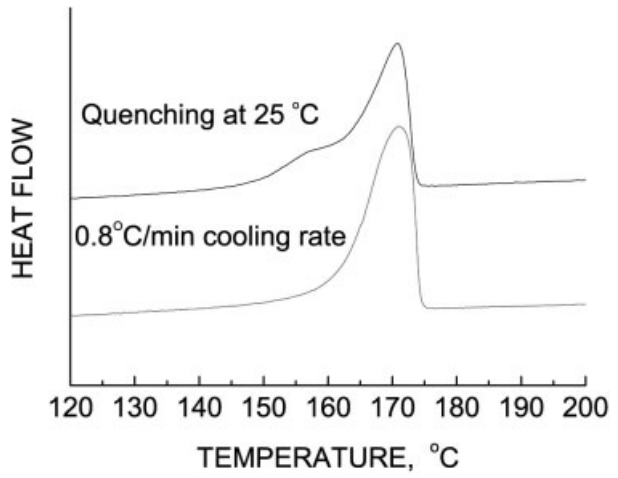

Figure 4 Ascending DSC curves of PVDF membrane by different cooling conditions. [Color figure can be viewed in the online issue, which is available at www.interscience.wiley.com.]

sile rate is 50 mm/min. For each specimen, three runs were performed.

DSC characterization of PVDF blend materials

A DSC (PerkinElmer, DSC-7) was used to determine the dynamic crystallization temperature for the dynamic phase diagram and other information of PVDF crystallization. About 10 mg solid sample, by weighing PVDF blend materials, was sealed in a DSC pan, melted, and kept at 220°C for 5 min to ensure complete melting and equilibration, and then cooled at 10°C/min to 25°C. The onset of the exothermic peak during the cooling was taken as the crystallization temperature. The heat of crystallization ΔH_c was determined from the exothermic peak area during cooling. Similar to the descending DSC, the ascending DSC was also obtained at 10°C/min heat rate, to demonstrate the effect of the cooling rate on membrane.

Morphology characterization of PVDF and its blend

DBP was extracted by ethanol and the membranes were fractured in liquid nitrogen. The cross-sectional morphologies of the membrane were observed using a scanning electron microscopy (SEM, Quanta 200, Netherlands FEI).

RESULTS AND DISCUSSION

Morphology of PVDF

Lloyd and his coworkers have studied in detail the method and process of formed membrane via TIPS, including the process of thermodynamics and kinemics.[11,19–33] Generally, TIPS process can proceed via either solid–liquid phase separation or liquid–liquid phase separation,[11,19] which can be represented in terms of a temperature–composition phase diagram. Solid–liquid phase separation usually results from the crystallization of the polymer from the homogeneous solution phase. The driving force for this phase separation is the difference in polymer chemical potential in the crystalline and solution phases. The crystallization kinetics of the polymer, and in some cases, the diluent play important roles on determining the structure from the solid–liquid phase separation.[21–23]

In this study, the crystallization curve for PVDF-DBP shown in Figure 1 confirms Lloyd's report,[11] which indicates that this system exhibits solid–liquid phase separation via polymer crystallization, at the indicated cooling rate, throughout the composition and temperature range of interest. No liquid–liquid phase separation is expected.

The membranes formed by different PVDF concentrations showed significant differences in morphology of membranes under the quenching condition. The typical scanning electron micrograph of the cross section of the membranes of two magnifications are shown in Figure 2. Spherulitic morphology was not clear for 20 and 30% PVDF membranes [Fig. 2(a, b)]. PVDF membranes with concentration in the range 40–60 wt % [Figs. 2(c–e)] presented the irregular spherulitic morphologies; moreover, the microvoids between spherulites (interspherulite) and smaller microvoids within spherulites (intraspherulite) were found. There was not much differences between the micrographs obtained from 50 and 60% PVDF membranes, so that the different magnifications for PVDF-60 were shown [Fig. 2(e)].

The spherulitic morphology results typically from solid–liquid phase separation via nucleation and growth of the polymer with accompanying rejection of the liquid diluent. It also presented in PP membrane.[11,20–22] But, the spherulitic morphology of the low concentration of PVDF (20 or 30 wt %) films is not as evident as that of the high concentration PVDF (40, 50, 60 wt %) films.

At the slow cooling rate, the morphologies of 40, 50, and 60 wt % PVDF membranes are shown in Figure 3. As compared with Figure 2, the spherulitic morphologies in the slow-cooled sample became more regular and larger. In addition, there are more spherulites

TABLE I
Melt Information of PVDF at Different Cooling Conditions

Cooling condition	Melt point (°C)	ΔH_m (J/g)
Quenching at 25°C	170.72	67.33
0.8°C/min	170.88	72.98

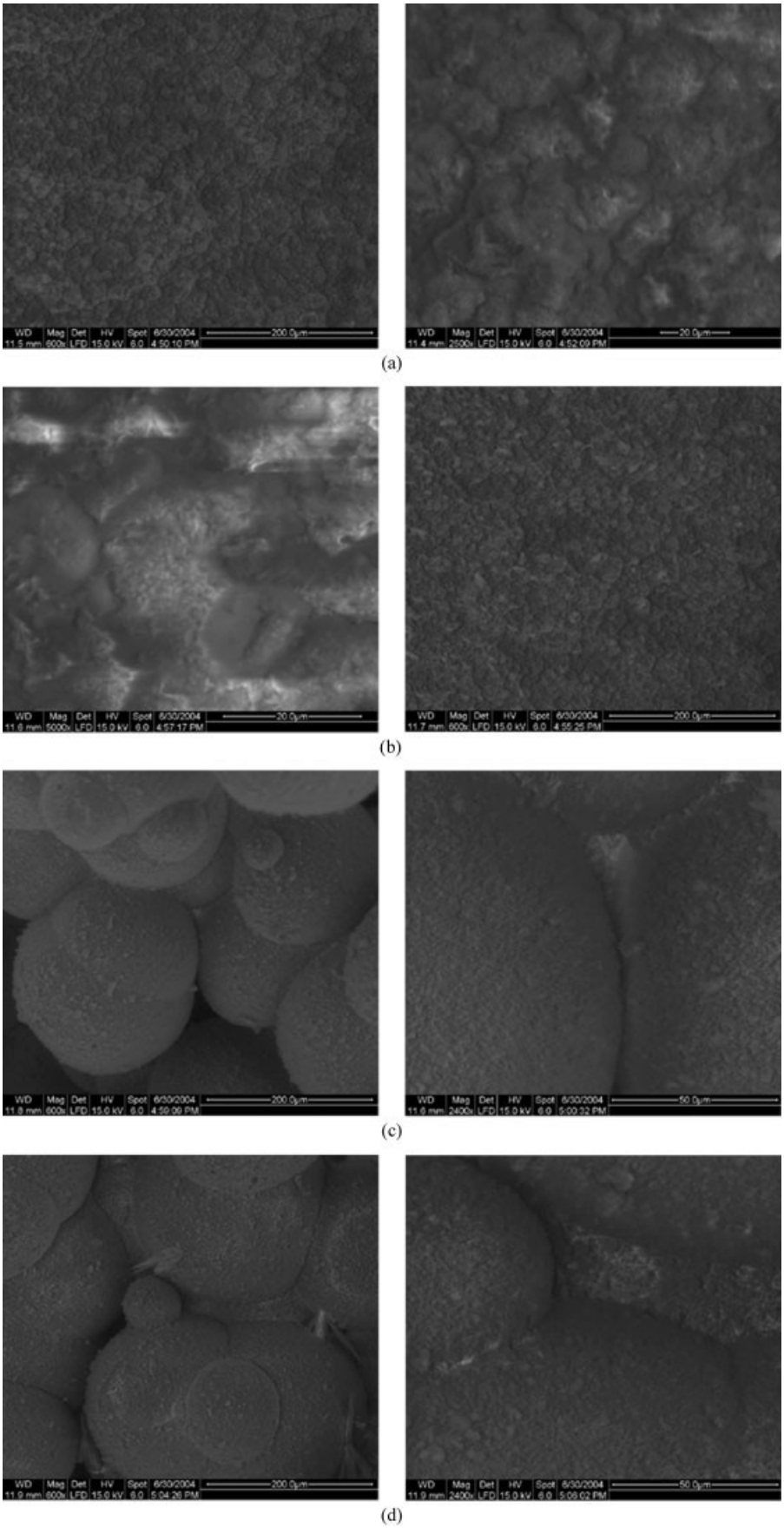

Figure 5 Morphology of the PVDF/$CaCO_3$ blend membranes, (a) a′: PVDF/$CaCO_3$/DBP = 34.3/16.7/50%; (b) b′: PVDF/$CaCO_3$/DBP = 40/20/40. Quenching at (a, b) 25°C; at (a′, b′) 0.8°C/min cooling rate.

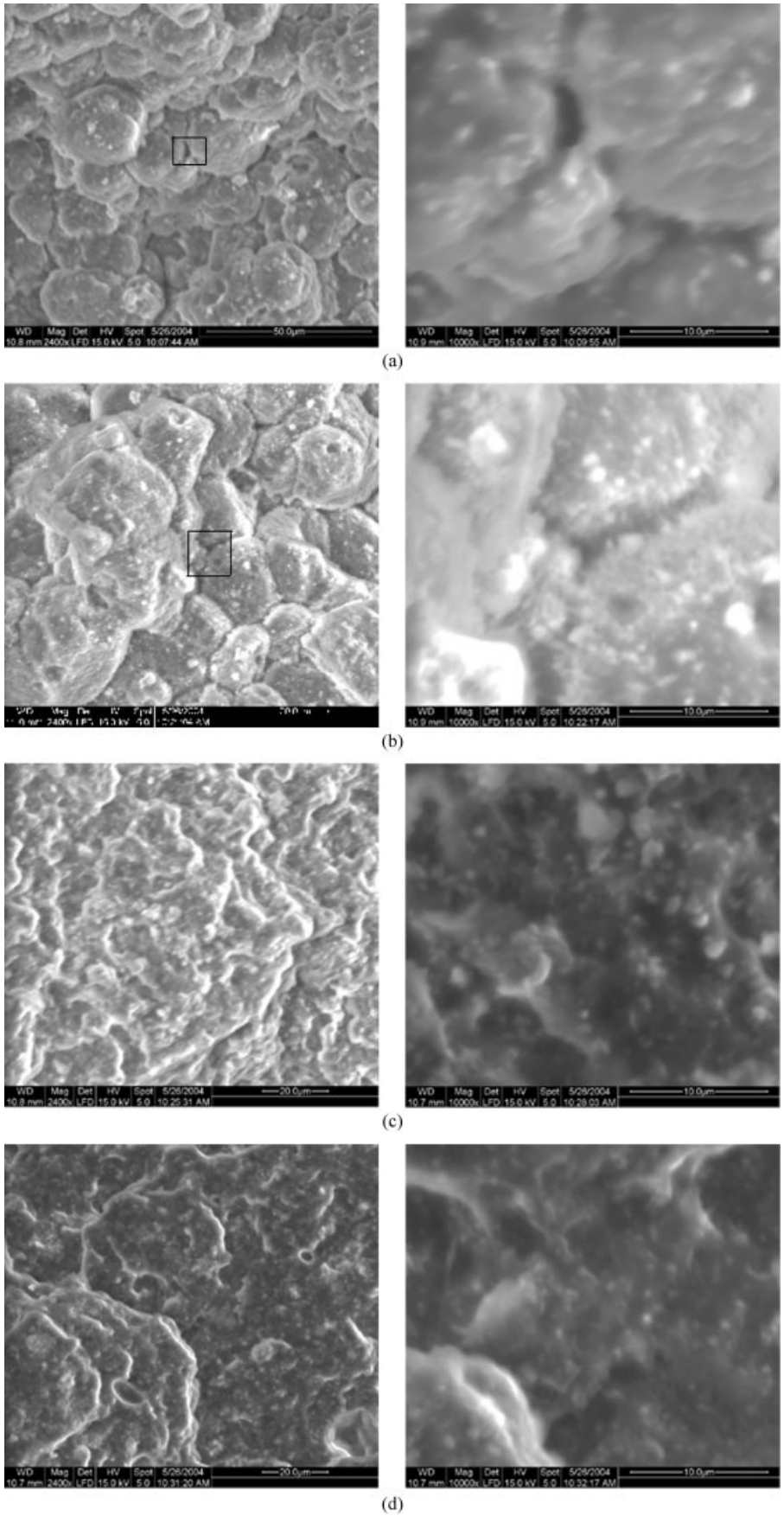

Figure 6 Effects of DBP on the morphology of blend membranes (ratio of PVDF/$CaCO_3$ is constant, DBP weight fraction, (a) 50%, (b) 40%, (c) 20%, (d) 0%).

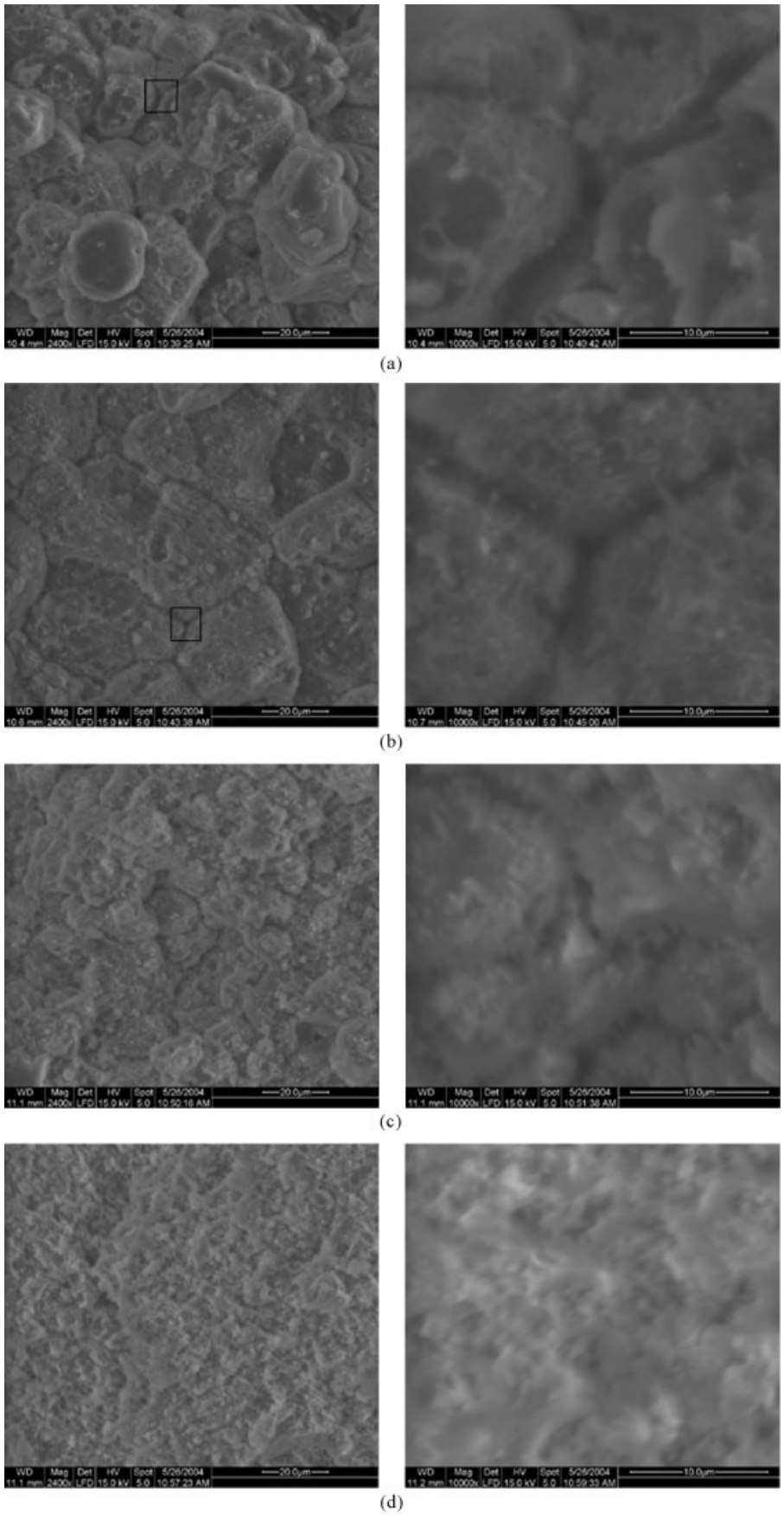

Figure 7 Effects of $CaCO_3$ on the morphology of the blend membranes ($CaCO_3$ weight fraction, (a) 7%, (b) 21%, (c) 35%, (d) 49%).

impinged with one another as the increase of PVDF concentration from 40 to 60 wt %, since the sample has relative great nucleation density when PVDF concentration increases.[27] Crystallization studies show[34] that the rate of cooling determines the number and size of crystallites, and slower cooling rates reduce the kinetics of crystallization, which gives a polymer chain more opportunity to disentangle during crystallization, increases the perfection of the crystals. Comparison of DSC curve forms shown in Figure 4 and crystallization heats summarized in Table I at different cooling conditions reveals more perfect crystal present in the slow-cooled sample, which provides a higher crystallization heat.

The increased spherulitic size and more regular shape (sphere) of the slow-cooled PVDF sample is indicative of the slower growth rate of nucleation and the less nucleation density in the sample prepared by nonisothermal TIPS, so that the spherulites in the 20 and 30 wt %PVDF samples are isolated from one another. Hence, the membranes, like dispersed sands, had no the structure integrality, and the scanning electron micrograph has not been obtained in this study.

Morphology of PVDF/$CaCO_3$ blend

The morphologies of the blend membranes from PVDF/$CaCO_3$/DBP shown in Figure 5 indicate the effects of the cooling condition on the morphology of blend membranes. Similar to PVDF membranes, at slow cooling rate, the blend membranes also present a regular, large, spherical morphology [Fig. 5(a, b)], This shows that a given $CaCO_3$ weight fraction is not enough to influence the aggregation and growth of crystals at the slow cooling rate, what is more, $CaCO_3$ were entrapped into the spheres, which makes the surface of spheres in the blend membranes coarser than that of spheres in the PVDF membranes. But, when compared with the same concentration PVDF membrane in Figure 2(c), in the quenched samples, no obvious spherulites are found [Fig. 5(b)] due to the introduction of $CaCO_3$ into PVDF/DBP solution. This reveals that at the quenching condition, the existence of $CaCO_3$ influences the aggregation and growth of crystal nuclei into the morphology as shown in Figure 2(c).

Comparison of Figures 2, 3, and 5 shows that the interspherulitic microvoids in the slow-cooled samples were much larger than those in the quenched samples regardless of PVDF membrane or PVDF blend membrane, since more diluent was rejected between PVDF spherulites during the slow crystallization process.

In the process of demonstrating the effects of the initial composition on the morphology of the blend membranes, the second (II) system of preparing blend membrane was adopted. In this practice process, the cooling rate is not calculated. But, only one parameter is variable, and the others are invariant.

TABLE II
Crystallization Heat and Temperature for the Blend Samples with Different $CaCO_3$ Weight Fraction

$CaCO_3$ content (%)	ΔH_{mb} (J/g), PVDF blends	ΔH_{mp} (J/g), PVDF	Peak temperature (°C)
7	38.23	60.68	134.60
21	31.44	64.16	131.40
35	22.21	63.46	126.70
49	12.99	61.86	122.55

Figures 6 and 7 shows the effects of initial composition on the morphology of blend membranes. As shown in Figure 5, with DBP weight fraction decreasing, the structure of blend membranes become dense, microvoid and spherulitic morphologies do not exist in the blend membrane of the low 20 wt % DBP weight fraction. The effects of $CaCO_3$ on the morphology of blend membrane shown in Figure 7 indicate that $CaCO_3$ play a very important role in the blend membrane morphology. As shown in Figure 7, with the increase of $CaCO_3$ weight fraction, the decrease of PVDF weight fraction, the morphology of spherulites becomes illegible gradually [Fig. 7(c)], even disappears [Fig. 7(d)]. The reason of morphology change is attributed to the hindrance of $CaCO_3$ to the aggregation of crystal nuclei or PVDF macromolecules. As a result, the spherulite cannot be formed, and the diluent is dispersed, which is a favorable morphology to separation membrane

The effects of $CaCO_3$ weight fraction on the crystallization of PVDF were further examined by DSC and summarized in Table II. The heat values in Table II shows that $CaCO_3$ weight fraction has no obvious influence on the crystallization heat or crystallinity, since it is well-known that the crystallization heat is a direct measure of the crystallinity of a polymer. But, the crystallization peak temperature shifts to the low temperature with increasing $CaCO_3$ weight fraction at a 10°C/min cooling rate. This reveals $CaCO_3$ weight fraction has a considerable influence on the crystallization kinetics of blend system.

Effect of DBP and $CaCO_3$ weight fraction on the tensile break strength of PVDF

The effect of DBP and $CaCO_3$ weight fraction on the tensile break strength of PVDF is shown in Figure 8. Evidently, both DBP and $CaCO_3$ have a negative effect on the tensile break strength of PVDF. With the increase of DBP and $CaCO_3$ weight fraction, the tensile break strength decreased. It is well-known that there is no strong affinity between PVDF and untreated

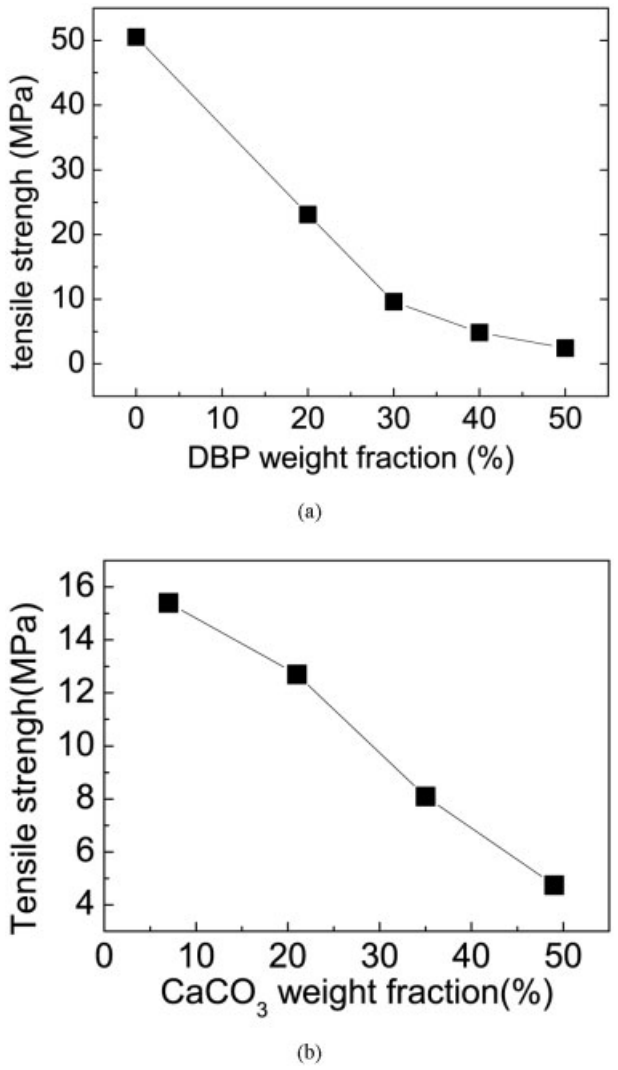

Figure 8 Effect of DBP and $CaCO_3$ weight fraction on the tensile break strength of PVDF.

$CaCO_3$ particle due to the low-surface energy of PVDF. Therefore, the mechanical property of PVDF was influenced by $CaCO_3$.

CONCLUSIONS

$CaCO_3$ weight fraction has no obvious influence on the crystallization heat of PVDF/DBP system. However, it has a considerable influence on the crystallization kinetics of blend system. As a result, $CaCO_3$ existence did not influence the formation of the large, spherulitic morphology of PVDF at a slow cooling rate condition, and at the quenching condition, the formation of the spherulitic morphology was disturbed by the introduction of $CaCO_3$. At a specified cooling rate, the morphology of PVDF film can be adjusted by the introduction of different $CaCO_3$ weight fraction. $CaCO_3$ had a negative effect on the tensile break strength of PVDF.

References

1. Wang, D. L.; Li, K.; Teo, W. K. J Membr Sci 1999, 163, 211.
2. Lin, D. J.; Chang, C. L.; Chen, T.-C.; Cheng, L.-P. Desalination 2002, 145, 25.
3. Lin, D. J.; Chang, C. L.; Huang, F. M.; Cheng, L.-P. Polymer 2003, 44, 413.
4. McGuire, K. S.; Lloyd, D. R.; Lim, G. B. A. J Membr Sci 1993, 79, 27.
5. Atkinson, P. M.; Lloyd, D. R. J Membr Sci 2000, 171, 1.
6. Matsuyama, H.; Okafuji, H.; Maki, T.; Teramoto, M.; Kubota, N. J Membr Sci 2003, 223, 119.
7. Song, S.-W.; Torkelson, J. M. J Membr Sci 1995, 98, 209.
8. Matsuyama, H.; Ohga, K.; Maki, T.; Tearamoto, M.; Nakatsuka, S. J Appl Polym Sci 2003, 89, 3951.
9. Luo, R.-L.; Young, T.-H.; Sun, Y.-M. Polymer 2003, 44, 157.
10. Yang, M.-C.; Perng, J.-S. J Polym Res 1999, 6, 251.
11. Lloyd, D. R.; Kinzer, K. E.; Tseng, H. S. J Membr Sci 1990, 52, 239.
12. Hamanaka Katsuhikok; Shimizu Tetsuo. S. Eur. Pat. 1,369,168 (2003).
13. Takamura Masakazu; Yoshida Hitoshi. U.S. Pat. 6,299,773 (2001).
14. Doi Yoshinao; Matsumura Haruo. U.S. Pat. 5,022,990 (1991).
15. Wara, N. M.; Francis, L. F.; Velamakanni, B. V. J Membr Sci 1995, 104, 43.
16. Genné, I.; Kuypers, S.; Leysen, R. J Membr Sci 1996, 113, 343.
17. Doyen, W.; Adriansend, W.; Molenbergs, B.; Leysen, R. J Membr Sci 1996, 113, 247.
18. Aerts, P.; Van Hoof, E.; Leysen, R.; Vankelecom, I. F. J.; Jacobs, P. A. J Membr Sci 2000, 176, 63.
19. Lloyd, D. R.; Kim, S. S.; Kinzer, K. E. J Membr Sci 1991, 64, 1.
20. Kim, S. S.; Lloyd, D. R. J Membr Sci 1991, 64, 13.
21. Lim, G. B. A.; Kim, S. S.; Ye, Q.; Wang, Y. F.; Lloyd, D. R. J Membr Sci 1991, 64, 31.
22. Kim, S. S.; Lim, G. B. A.; Alwattari, A. A.; Wang, Y. F.; Lloyd, D. R. J Membr Sci 1991, 64, 41.
23. Alwattari, A. A.; Lloyd, D. R. J Membr Sci 1991, 64, 55.
24. Kim, S. S.; Lloyd, D. R. Polymer 1992, 33, 1026.
25. Kim, S. S.; Lloyd, D. R. Polymer 1992, 33, 1036.
26. Kim, S. S.; Lloyd, D. R. Polymer 1992, 33, 1047.
27. Lim, G. B. A.; Lloyd, D. R. Polym Eng Sci 1993, 33, 529.
28. Lim, G. B. A.; Lloyd, D. R. Polym Eng Sci 1993, 33, 537.
29. Laxminarayan, A.; McGuire, K. S.; Kim, S. S.; Lloyd, D. R. Polymer 1994, 35, 3060.
30. Song, S.-W.; Torkelson, J. M. Macromolecules 1994, 27, 6389.
31. McGuire, K. S.; Laxminarayan, A.; Lloyd, D. R. Polymer 1995, 36, 4951.
32. Matsuyama, H.; Berghmans, S.; Lloyd, D. R. Polymer 1999, 40, 2289.
33. Matsuyama, H.; Berghmans, S.; Batarseh, M. T.; Lloyd, D. R. J Membr Sci 1998, 142, 27.
34. Ludwig, B. W.; Urban, M. W. Polymer 1997, 38, 2077.